

AUTOMATIC FEATURE EXTRACTION FROM PLANETARY IMAGES

Giulia Troglio^{1,2}, Jacqueline Le Moigne³, Jon A. Benediktsson¹, Gabriele Moser², Sebastiano B. Serpico²

¹ University of Iceland, Faculty of Electrical and Computer Engineering, Reykjavik (Iceland), e-mail: giulia.troglio@unige.it

² University of Genoa, Dept. of Biophysical and Electronic Engineering, Genoa (Italy)

³ Goddard Space Flight Center, Software Engineering Division, NASA GSFC Code 580, Greenbelt MD, USA

ABSTRACT

With the launch of several planetary missions in the last decade, a large amount of planetary images has already been acquired and much more will be available for analysis in the coming years. The image data need to be analyzed, preferably by automatic processing techniques because of the huge amount of data. Although many automatic feature extraction methods have been proposed and utilized for Earth remote sensing images, these methods are not always applicable to planetary data that often present low contrast and uneven illumination characteristics. Different methods have already been presented for crater extraction from planetary images, but the detection of other types of planetary features has not been addressed yet. Here, we propose a new unsupervised method for the extraction of different features from the surface of the analyzed planet, based on the combination of several image processing techniques, including a watershed segmentation and the generalized Hough Transform. The method has many applications, among which image registration and can be applied to arbitrary planetary images.

Index Terms— Crater Detection, Feature Extraction, Watershed Segmentation, Hough Transform.

1. INTRODUCTION

The Lunar Reconnaissance Orbiter (LRO) is a NASA mission, aimed at creating a comprehensive atlas of the features and resources of the Moon to prepare exploration and scientific missions to the Moon and to study its environment [1]. Having officially reached lunar orbit on June 23rd, 2009, LRO has now marked one full year on its mission of scouting the Moon. In only the first year of the mission, LRO has gathered more digital information than any previous planetary mission in history. Different types of data are being collected by LRO at different times, by different sensors, and from different view-points: Multitemporal, multimodal and stereo-images will be soon available. Therefore, image registration will be an essential task to jointly exploit, integrate, or compare all

these different data. Feature extraction, i.e., extraction of spatial features in the images, is the first step in the image registration process. Furthermore, the feature extraction is important for further analysis of the data.

Identification of spatial features on planetary surfaces can be manually performed by human experts but this process can be very time consuming. Therefore, a reliable automatic approach to detect the position, structure, and dimension of each feature is highly desirable. This is a difficult task for several reasons: Limited data are usually available, the quality of the images is generally low (i.e., it depends on illumination, surface properties and atmospheric state), and the features that are present in the images can be barely visible due to atmospheric erosion and they may be based on different structure types of variable sizes.

Among the typical features in planet-surface imagery, craters play a primary role. Detection of craters has been widely addressed and different approaches have recently been proposed in the literature, based on the analysis of planetary topography data [2], satellite images [3] in the visible spectrum and the infrared spectrum. Here, we focus on optical image-based approaches for crater and rock detection. Different approaches have been presented, based on template matching [3], [4], [5], texture analysis [6], neural networks [7], [8], boosting approaches [9], or a combination of these techniques [10], [11]. In particular, in [12], the identification of impact craters was achieved through the analysis of the probability volume created as a result of a template matching procedure. Such methods enable the identification of round spatial features with shadows. Kim and Muller [6] presented a crater detection method based on texture analysis and ellipse fitting. That method was not robust when applied to optical images, hence it was performed by using fusion techniques exploiting both DEM and optical images. In subsequent work [13], in order to automatically detect craters on Mars, the authors proposed a combination of edge detection, template matching, and supervised neural network-based schemes for the recognition of false positives. In a different approach, Martins et al. [14] adopted a super-

vised boosting algorithm, originally developed by Viola and Jones [15] in the context of face detection, to identify craters on Mars. In [16], Urbach and Stepinski presented a different approach for crater detection in panchromatic planetary images. The method in [16] is based on using mathematical morphology for the detection of craters and on supervised machine learning techniques to distinguish between objects and false alarms. Until now, apart from craters, no other types of planetary features have been addressed in the literature.

In order to overcome the typical problems of planetary images with a lack of contrast, poor illumination, and a lack of good features, we propose here a new unsupervised region-based approach for the extraction of different planetary features. The main contribution of this paper is a novel unsupervised method for the segmentation of planetary images, aimed at extracting not only craters but also other planetary features. Moreover, the approach allows not only to locate the features, but also to reconstruct their shape.

The proposed feature extraction approach is described in Section 2. Section 3 includes the presentation and analysis of the obtained results. In the same section, the application of the proposed technique to an image registration process is presented. Experimental results are shown with images representing the surface of Mars, because LRO images are not available yet. Finally, conclusions and ideas for future improvements are presented in Section 4.

2. THE PROPOSED APPROACH

Planetary images show the surface of a planet and its structures. The aim here is to automatically detect the different structures that are present on a considered planetary surface by using image analysis techniques. The extracted features could then be used for image registration registration purposes, as will be shown in Section 3. Different types of features are present in the planetary images, and their size, shape and position are estimated by applying different methods.

The main features to be extracted are craters and rocks. Craters are objects of approximately elliptical shape with shadows, due to their depth and uneven illumination. Rocks have small circular or elliptical shape, with almost no shadows. The extraction of these spatial features is a difficult task, because planetary images are blurry, quite noisy, present lack of contrast and uneven illumination, and the represented objects are not well defined. For these reasons, a region-based approach, based on segmentation, has been chosen in order to address such problems. Segmentation is the process of partitioning an image into multiple regions, for instance, in order to distinguish objects from the background. A frequent approach to segmentation introduces a set of characteristic points that are related to the objects to be detected, automatically selected and used as “seed points” to segment the images. Many segmentation approaches have been explored in the literature. Here, the watershed algorithm, presented

by Beucher in [17], has been chosen, a method which is automatic, robust and fast. The basic concept of watershed segmentation is visualizing a grey-level image into its topographic representation (i.e., the grey level of a pixel represents its elevation). A flooding process starts from the minima of the image, so that the merging of the flooding coming from different sources is prevented. As a result the image is partitioned into two different sets: The catchment basins (i.e., the regions) and the watershed lines (i.e., the region boundaries). The flowchart of the proposed technique for spatial feature extraction is shown in Figure 1.

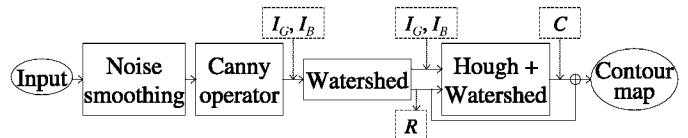


Fig. 1. Flowchart of the proposed approach.

Before applying feature extraction techniques, the images need to be preprocessed. First, the noise is smoothed by applying Gaussian filtering and median filtering operations in cascade [18]. Then, in order to detect edges, the image gradient is computed by using the Canny edge detector [19]. As an intermediate result of this operation an intensity gradient, I_g , is generated. Then, by applying a non-maximum suppression algorithm followed by an hysteresis thresholding to I_g , a binary gradient image, I_b , is obtained but this image shows the contours of the objects represented in the original image.

Rocks generally appear like closed contours in I_b , because of the absence of shadows. In order to extract these features, the watershed segmentation algorithm is applied to I_b and closed contours are extracted. All the areas included within a closed contour correspond to “seed point-areas,” and are identified as regions. The result of this first step is a binary image R that shows the rock boundaries.

While rocks appear like closed contours and can be easily detected, craters have a more complex structure and, due to their depth and uneven illumination, exhibit shadows. Their borders can be approximated with incomplete non-continuous elliptical curves. A generalized Hough accumulator [20] is used to identify the seed points to detect these structures from I_b . For every pair of pixels that are detected as edge points in I_b and exhibit opposite gradient directions, an accumulator, corresponding to the median point between them in the image plane, is incremented of a unit value. The maxima of the accumulator are taken as centers of ellipses. The three parameters describing the ellipse centered in each detected maximum are then computed and a 3D accumulator is used to estimate the two semi-axes and the direction angle of the ellipse from all the pairs of points that contributed to the accumulator in the considered center. The center of each ellipse that has been generated is used as a seed point for segmentation. Starting from all the detected seed points, a watershed

algorithm is applied to I_g and the craters are identified. I_g is used here because it represents not only the edges but also the elevation information. As a result, a binary image C that shows the crater boundaries is obtained. A binary image, I_c , which represents the contours of all detected features, is created. The binary image, I_c , shows the boundaries of the features, identifies their location and estimates their shape.

The proposed technique for feature extraction can be used to register image pairs representing the same scene. For registration, two binary images need to be extracted from both images to be registered and their match can be estimated (in Section 3 the proposed approach to image registration is presented).

3. EXPERIMENTAL RESULTS

Since LRO images are not yet available, experiments were carried out using Mars data, collected during the 2001 Mars Odyssey mission, by the THERMAL EMISSION IMAGING SYSTEM (THEMIS), an instrument on board the Mars Odyssey spacecraft. Such an instrument combines a 5-band visual imaging system with a 10-band infrared imaging system [21]. Both visible (VIS) and infrared (IR) images, with a resolution of 18 meters and 100 meters per pixel, respectively, were used to test the proposed approach. For the experiments 5 VIS and 7 IR images were selected.

Reference data were generated by manually analyzing each image of the data set and identifying all the craters and rocks that are present. Only objects completely included within the images were considered (i.e., objects cut by the borders of the image were discarded). No limits were imposed on the minimum dimensions of the features to be detected. A quantitative assessment of the obtained results by the proposed method was performed using these reference data. This was accomplished by comparing the obtained results with the labeled features in the correspondent reference map, RM . The Detection percentage D , the Branching factor B , and the Quality percentage Q were computed as follows:

$$D = \frac{100 * TP}{TP + FN}; B = \frac{FP}{TP}; Q = \frac{100 * TP}{TP + FP + FN}; \quad (1)$$

where True Positive (TP) is the number of detected features that correspond to labeled objects in RM , False Positive (FP) is the number of features detected by the proposed approach, which do not correspond to any object in RM , and False Negative (FN) is the number of objects in RM that have not been detected by the proposed approach. The global values of D , B , and Q and the total number of TP , FP , and FN obtained by the proposed approach both for VIS and IR data are shown in Table 1. The global values of D for VIS data and IR data were about 82% and 78%, respectively; these high values indicate a good detection rate (because of the high number of TP). B was about 0,03 for VIS and 0,05 for IR, which indicate a small amount of false detections with

Table 1. Average numerical performance of the proposed approach as measured by Detection percentage (D), Branching factor (B) and Quality percentage (Q) and total number of True Positive (TP), False Positive (FP) and False Negative (FN) detections on visible and infrared images, respectively.

Data	D	B	Q	TP	FP	FN
VIS	82%	0,03	81%	197	6	58
IR	78%	0,05	75%	211	6	61

respect to the true detections in both cases, thanks to the small number of FP . The detection performance of the proposed approach in terms of D , B , and Q compares favorably with most of the results previously published for automatic crater detection methods [13, 16, 22]. Nevertheless, no full comparison is possible, since all the other methods are based on using only crater features.

Visual results are shown for a partition of a single band VIS image (Figure 2-a). The grey level image is first pre-

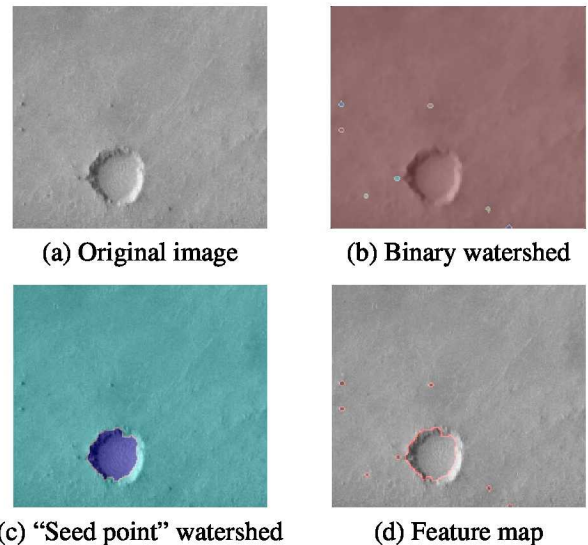


Fig. 2. Experimental results obtained by applying the proposed method to a VIS image. (a) Original image, (b) watershed segmentation applied to I_b , (c) watershed segmentation, using the maxima of the Hough accumulator as “seed points”, and (d) detected features. Each color in the segmentation map denotes a different region.

processed by a smoothing filter in order to reduce the noise. The Canny operator is applied to the smoothed image. Subsequently, in order to extract the rocks, a watershed algorithm is applied to the binary image gradient I_b . Rock segmentation results are shown in Figure 2-b. Then, the generalized Hough transform is computed and a watershed segmentation is applied, starting the flooding process from the ellipse centers and leading to the detection of the craters. The segmentation

result are shown in Figures 2-c. Finally, the extracted features, including both rocks and craters, are combined into a binary map and shown in 2-d, transparently superimposed to the original image. By a visual inspection, it is possible to appreciate the accuracy of both the detection and the reconstruction of the feature shape.

Visual results are also shown for a partition of the first band of an IR image (Figure 3-a). Figure 3-b shows the seg-

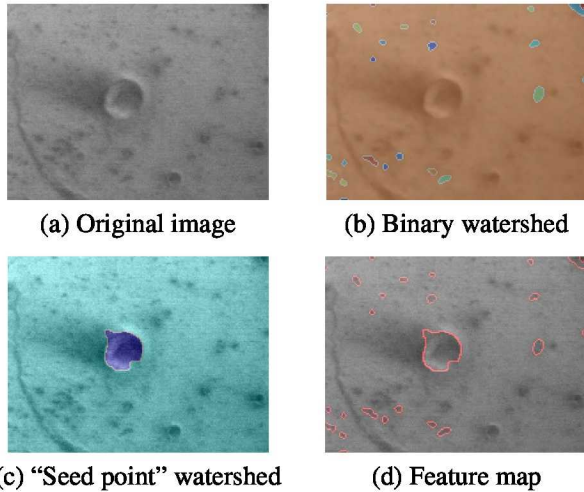


Fig. 3. Experimental results obtained by applying the proposed method to the first band of an IR THEMIS image.

mentation results when watershed is applied to I_b . Figure 3-c shows the crater segmentation results. The different extracted features are combined and shown in 3-d. In this example, not all the features are detected. This is because their contours were not extracted by the Canny operator. An improvement of the edge detection step may improve the accuracy of the method and it is currently under investigation. Anyway, we will show below that the detected features are enough to achieve an accurate registration.

To demonstrate the applicability of the proposed method to registration, two different non-registered bands of an IR image are used. In order to show the results, the same partition of Figure 3-a is used; in particular, the 4^{th} and 5^{th} bands were selected (Figures 4-a and 4-b, respectively). For both band images, craters and rocks are detected and their contours are extracted and represented in binary contour images, $I_{c,1}$ and $I_{c,2}$, as shown in Figures 4-c and 4-d, respectively. The rotation and translation between the two bands are visible by looking at Figure 4-e, in which the two non-registered contour images are superimposed in a false-color representation. The contours extracted from the 4^{th} band image, $I_{c,1}$, are represented in green, whereas the 5^{th} -band contours, $I_{c,2}$, are shown in red. The registration scheme used in this phase was based on a global optimization technique aimed at estimating the optimum parameters of an image transformation model. The contour images, which represent the features of

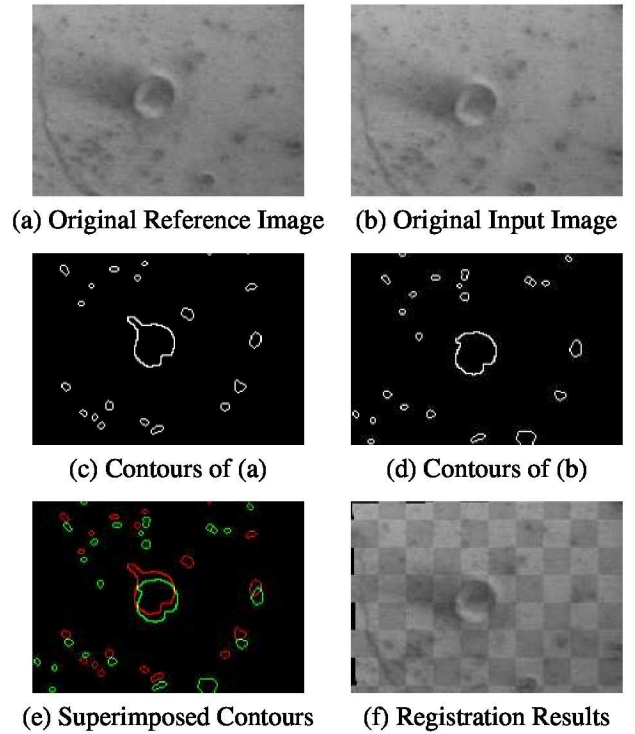


Fig. 4. Registration results for a partition of (a) the 4^{th} and (b) the 5^{th} bands of an IR image. (c) and (d) feature contours extracted from (a) and (b), respectively. (e) Contour images superimposed and represented in a false-color composition (i.e., the green plane is (c), the red plane is (d), and the blue plane is identically zero). (f) Registration results, by using a checkerboard representation.

the two input image bands, were fed as inputs to an optimization module. The transformation matrix was to be optimized: Its goodness was evaluated by an objective function and its optimization was achieved by applying a genetic algorithm [23]. After the optimum matrix was estimated, it was used to transform and interpolate one of the two bands with respect to the other one. The co-registered bands are shown in Figure 4-f, by using a checkerboard representation: Each tile of the board represents the registered input band and the reference band, alternately. The registration accuracy can be evaluated by looking at the continuity of the features at the borders of the tiles. The visual analysis of Figure 4-f suggests that the registration performed very well; craters and ridges appear continuous at the borders, i.e., the points of overlap.

4. CONCLUSIONS

In this letter a novel unsupervised region-based approach has been proposed for automatic detection of spatial features that characterize planetary surfaces. The proposed approach has been applied to the registration of planetary data.

The features to be extracted are not as well contrasted nor defined as for Earth data. However, small rocks, which are not affected by uneven illumination, can easily be detected by the proposed approach. Crater detection is more difficult than the rock detection, because of their depth and spatial extent and, consequently, their contours are often blurry and not continuous. Nevertheless, we showed here that their identification can be achieved and the proposed approach provided quite accurate results. The accuracy of the detection has been assessed by comparison to a manually generated reference map. The results in terms of several indices based on true and false positives compared favorably to previously proposed approaches. Moreover, we showed that the extracted features can be used to accurately register pairs of image bands acquired from the same sensor. The accuracy of the registration step is confirmed by visual inspection of the results.

The proposed approach represents the first important step for many applications dealing with all the various data that are being collected by LRO and other planetary missions, among which image registration and image analysis, with the aim of selecting safe landing sites, identifying lunar resources, and preparing for subsequent explorations of the Moon and Mars by both robots and humans.

In our future work we plan to integrate the shadow information around the features in order to improve the reliability of the edge detection and reduce the false alarms in the contour map I_c . The approach will be extended to the registration of multisensor images.

Acknowledgment

This research was supported by the Research of Fund of the University of Iceland and was performed at NASA Goddard Space Flight Center.

5. REFERENCES

- [1] "Lunar reconnaissance orbiter," Nasa facts, Goddard Space Flight Center, NASA, 2009.
- [2] G. Salamuniccar and S. Loncaric, "Method for crater detection from martian digital topography data using gradient value/orientation, morphometry, vote analysis, slip tuning, and calibration," *IEEE Trans. on Geoscience and Remote Sensing*, vol. 48, pp. 2317–2329, 2010.
- [3] A. Flores-Mendez, *Crater Marking and Classification using Computer Vision*, vol. 2905, Springer-Verlag, New York, 2003.
- [4] G. Michael, "Coordinate registration by automated crater recognition," *Planetary Space Sci.*, vol. 51, pp. 563–568, 2003.
- [5] T. Barata, E. I. Alves, J. Saraiva, and P. Pina, *Automatic Recognition of Impact Craters on the Surface of Mars*, vol. 3212, Springer-Verlag, Berlin, Germany, 2004.
- [6] J. R. Kim and J.-P. Muller, "Impact crater detection on optical images and DEM," in *ISPRS Extraterrestrial Mapping Workshop "Advances in Planetary Mapping"*, Houston, TX, 2003.
- [7] A. A. Smirnov, "Exploratory study of automated crater detection algorithm," Tech. rep., Boulder, CO, 2002.
- [8] P. G. Wetzler, B. Enke, W. J. Merline, C. R. Chapman, and M. C. Burl, "Learning to detect small impact craters," in *7th IEEE Workshops on Applications of Computer Vision*, 2005, vol. 1, pp. 178–184.
- [9] R. Martins, P. Pina, J. S. Marques, and M. Silveira, "A boosting algorithm for crater detection," in *Visualization, Imaging, Image Processing Conference*, Spain, 2008.
- [10] Y. Sawabe, T. Matsunaga, and S. Rokugawa, "Automated detection and classification of lunar craters using multiple approaches," *Advances Space Research*, vol. 37, no. 1, pp. 21–27, 2006.
- [11] J. Earl, A. Chicarro, C. Koeberl, P. G. Marchetti, and M. Milsen, "Automatic recognition of crater-like structures in terrestrial and planetary images," in *36th Annual Lunar and Planetary Science Conference*, Texas, 2005.
- [12] L. Bandeira, J. Saraiva, and P. Pina, "Impact crater recognition on mars based on a probability volume created by template matching," *IEEE Trans. on Geoscience and Remote Sensing*, vol. 45, pp. 4008–4015, 2007.
- [13] J. R. Kim, J.-P. Muller, S. van Gasselt, J. G. Morley, and G. Neukum, "Automated crater detection, a new tool for mars cartography and chronology," *Photogrammetric Engineering and Remote Sensing*, vol. 71, no. 10, pp. 1205–1217, 2005.
- [14] R. Martins, P. Pina, J. S. Marques, and M. Silveira, "Crater detection by a boosting approach," *IEEE Geoscience and Remote Sensing Letters*, vol. 6, pp. 127–131, 2009.
- [15] P. Viola and M. Jones, "Robust real-time face detection," *Int. Journal of Computer Vision*, vol. 57, pp. 137–154, 2004.
- [16] E. R. Urbach and T. F. Stepinski, "Automatic detection of sub-km craters in high resolution planetary images," *Planetary and Space Science*, vol. 57, pp. 880–887, 2009.
- [17] S. Beucher, "The watershed transformation applied to image segmentation," *Scanning Microscopy Int.*, vol. 6, 1992.
- [18] L. G. Shapiro and G. C. Stockman, *Computer Vision*, Prentice Hall, 2001.
- [19] J. Canny, "A computational approach to edge detection," *IEEE Trans. on Pattern Analysis and Machine Intelligence*, vol. 10, no. 6, 1986.
- [20] S. Tsuji and F. Matsumoto, "Detection of ellipses by a modified hough transformation," *IEEE Trans. on Computers*, vol. 27, 1978.
- [21] P. Christensen, B. M. Jakosky, H. H. Kieffer, M. C. Malin, H. Y. Mcsween, K. Nealson, G. L. Mehalland S. H. Silverman, S. Ferry, M. Caplinger, and M. Ravine, "The thermal emission imaging system (themis) for the mars 2001 odyssey mission," *Space Science Reviews*, vol. 100, pp. 85–130, 2004.
- [22] B. D. Bue and T. F. Stepinski, "Machine detection of martian impact craters from digital topography data," *IEEE Trans. on Geoscience and Remote Sensing*, vol. 45, pp. 265–274, 2007.
- [23] Z. Michalewicz, *Genetic Algorithms + Data Structures = Evolution Programs*, Springer Verlag, Berlin, third edition, 1999.